Biophysical Chemistry 301 (2023) 107082

Contents lists available at ScienceDirect

Biophysical Chemistry

journal homepage: www.elsevier.com/locate/biophyschem

Effects of curcumin in the interaction with cardiolipin-containg lipid monolayers and bilayers

Erika Aloi [a,1], Caterina M. Tone [a,b,1], Riccardo C. Barberi [a,b], Federica Ciuchi [b,*], Rosa Bartucci [c,*]

[a] Department of Physics, University of Calabria, 87036 Rende, Italy
[b] CNR Nanotec c/o Department of Physics, University of Calabria, 87036 Rende, Italy
[c] Department of Chemistry and Chemical Technologies, University of Calabria, 87036 Rende, Italy

ARTICLE INFO

Keywords:
Curcumin, Cardiolipin
DMPC
Lipid bilayers
Langmuir monolayers
AFM

ABSTRACT

Curcumin, a plant polyphenol extracted from the Chinese herb turmeric, has gained widespread attention in recent years because of its multifunctional properties as antioxidant, antinflammatory, antimicrobial, and anticancer agent. Effects of the molecule on mitochondrial membranes properties have also been evidenced. In this work, the interaction of curcumin with models of mitochondrial membranes composed of dimyristoylphosphatidylcholine (DMPC) or mixtures of DMPC and 4 mol% tetramyristoylcardiolipin (TMCL) has been investigated by using biophysical techniques. Spectrophotometry and fluorescence allowed to determine the association constant and the binding energy of curcumin with pure DMPC and mixed DMPC/TMCL aqueous bilayers. The molecular organization of pure DMPC and cardiolipin-containing Langmuir monolayers at the air-water interface were investigated and the morphology of the monolayers transferred into mica substrates were characterized through atomic force microscopy (AFM). It is found that curcumin associates at the polar/apolar interface of the lipid bilayers and the binding is favored in the presence of cardiolipin. At 2 mol%, curcumin is well miscible with lipid monolayers, particularly with mixed DMPC/TMCL ones, where compact terraces formation characterized by a reduction of the surface roughness is observed in the AFM topographic images. At 10 mol%, curcumin perturbs the stability of DMPC monolayers and morphologically are evident terraces surrounded by cur aggregates. In the presence of TMCL, very few curcumin aggregates and larger compact terraces are observed. The overall results indicate that cardiolipin augments the incorporation of curcumin in model membranes highlighting the mutual interplay cardiolipin-curcumin in mitochondrial membranes.

1. Introduction

Curcumin (Cur), a natural polyphenol extracted from the rhizome of *Curcuma longa*, is the primary bioactive component of turmeric powder and it has a characteristic yellow color [1]. It is used in various technological fields, ranging from food industry, where it is employed as a spice, to textile manufacturing where it acts as a pigment, from traditional medicine to pharmaceutical industry as a drug [2,3]. Over time, a broad spectrum of health benefits joint to low toxicity has been attributed to Cur in humans, including antioxidant and anti-inflammatory as well as antineoplastic activities [4–8].

From a chemical standpoint, Cur is a water-insoluble, lipophilic molecule whose structure consists of two phenyl rings, substituted with both hydroxyl and methoxyl oxide groups, connected via a seven carbon keto-enol linker (see Fig. 1). In spite of the fact that Cur is currently successfully administered for the treatment of different physiopathologies, its use is hampered by the low solubility and rapid degradation that make the molecule scarcely bioavailable. These limitations can be overcome by incorporating the polyphenol in bio-carriers, which include proteins and lipid aggregates such as monolayers, vesicles, and micelles, thus enhancing solubility and biodistribution [9]. A number of studies regarding the association of curcumin with lipid assemblies have demonstrated that the molecule affects the lipid structure and dynamics and perturbs membrane properties [10–19]. Moreover, the lipid composition plays a key role in determining the extent of the effects produced by curcumin on membranes. A specific lipid that interacts with curcumin is cardiolipin (CL), a unique lipid found in the membrane of mitochondria ([20] and references therein, [21]). In fact, effects of

* Corresponding authors.
E-mail addresses: federica.ciuchi@cnr.it (F. Ciuchi), rosa.bartucci@fis.unical.it (R. Bartucci).
[1] these authors contributed equally.

https://doi.org/10.1016/j.bpc.2023.107082
Received 11 June 2023; Received in revised form 21 July 2023; Accepted 30 July 2023
Available online 1 August 2023
0301-4622/© 2023 The Authors. Published by Elsevier B.V. This is an open access article under the CC BY license (http://creativecommons.org/licenses/by/4.0/).

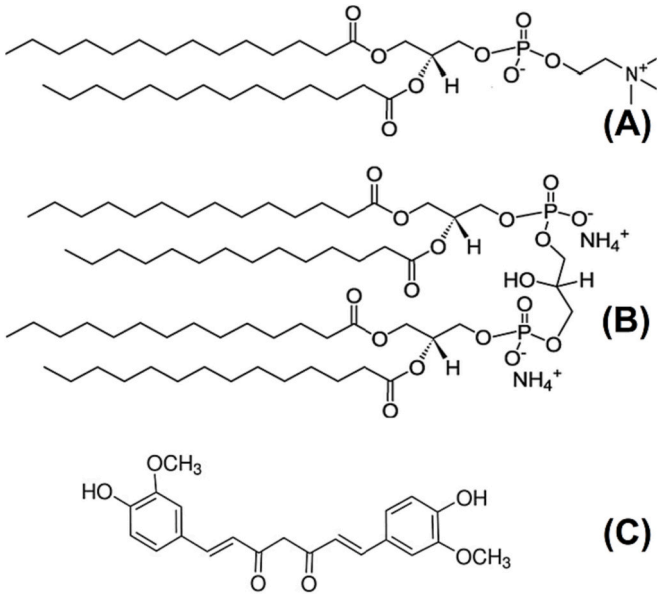

Fig. 1. Molecular structure of the lipids (A) DMPC and (B) TMCL, and of (C) curcumin.

curcumin on mitochondrial membranes and their models have been reported in a few recent studies [14,16,22–24]. Moreover, curcumin is rapidly accumulated in the endoplasmic reticulum (ER) and in lysosomes [25], having an impact on both ER stress and mitochondria functional pathways [24,26]. It is worth mentioning that the role of the ER stress in several pathological conditions, such as cancer, neurodegenerative and metabolic disorders, and the potential protection effect of curcumin against the development, or at least the slowing of the progression of such diseases, have been suggested by various researchers (see, e.g., [27] and references therein). For example, curcumin has been reported to induce ER stress-associated apoptosis and/or autophagy of many types of cancer cells through mitochondria-related events. These latter include DNA damage, disruption of intracellular calcium homeostasis, selective generation of reactive oxygen species as well as alteration of the mitochondrial membrane potential, mitochondrial dysfunction and unfolded protein response. Moreover, in the case of lymphocytes T, which are crucial in achieving a regulated effective immune response to pathogens, a modulation of ER stress by curcumin has been reported to induce either cell survival or cell death in various lymphocyte T-mediated autoimmune diseases, such as multiple sclerosis and rheumatoid arthritis. This is due to curcumin capacity to enhance the induction of unfolded protein response components in activated human T cells [26]. Therefore, comparative study on the impact of Cur on CL-free and CL-containing lipid membranes is of great interest to shed light on the mutual influence between Cur and CL in perturbing the membrane properties.

In this work, we present a biophysical study on the interaction of curcumin with membrane model systems in the form of fully hydrated bilayers and Langmuir monolayers. We aim at gain insight into the role of CL in modulating the influence of Cur on molecular properties of the lipid assemblies. To this end, we considered model systems of dimyristoylphosphatidylcholine (DMPC) and mixtures of DMPC and low amounts (4 mol%) of tetramyristoylcardiolipin (TMCL). DMPC is a bilayer-forming lipid having a zwitterionic phosphocholine head group and a hydrocarbon region of two symmetrical saturated chains with 14 carbon atoms. TMCL is a lipid having two phosphatidyl moieties joined by one glycerol molecule: it has a relatively small anionic headgroup and a large hydrophobic domain formed by four myristoyl chains (see Fig. 1). This molecular architecture renders cardiolipin capable of forming inverted hexagonal structures in isolation under certain conditions (for example, at low pH and in the presence of divalent cations) [28]. Mixtures of DMPC and low amount of TMCL form bilayers [28,29] that can be considered a mimic of mitochondrial membranes of eukarya [20]. Although the chains of CL in eukaryotic mitochondria are primarily unsaturated, we investigated mixtures of DMPC and TMCL with identical C14:0 chains to rule out hydrophobic mismatch in discussing our results, as CL content and fatty acyl composition differentially target membrane physical properties [30].

The solvatochromic properties of curcumin in various solvents and in DMPC and DMPC/TMCL bilayers as well as its binding constant to the lipid membranes have been evaluated by spectrophotometry and intrinsic fluorescence. Moreover, the interactions among the components (i.e., lipid-lipid and lipids-Cur) have been investigated on Langmuir monolayers of pure DMPC and mixed DMPC/TMCL lipids, without and with curcumin. Further, the morphology of thin films produced by depositing the monolayers onto freshly cleaved mica substrates have been studied with Atomic Force Microscopy (AFM). How TMCL modulates the interaction of Cur with model membranes is presented and discussed.

2. Materials and methods

2.1. Chemicals

The synthetic lipids DMPC (1,2-dimyristoyl-sn-glycero-3-phosphocholine) and TMCL (1′,3′-bis[1,2-dimyristoyl-sn-glycero-3-phospho]-glycerol) were from Avanti Polar Lipids (Birmingham, AL, USA). Curcumin (4-hydroxy-3-(3-oxo-1-phenylbutyl)-coumarin) was purchased from Sigma-Aldrich (St. Louis, MO, USA). Dulbecco's phosphate-buffered saline (DPBS, 10 mM, pH 7.4) was from Sigma-Aldrich and Milli-Q grade deionized water from Millipore. All the chemicals were used as provided, without any further purification.

2.2. Spectrophotometry

UV–Vis measurements were carried out either on curcumin in various solvents at 15 μM or on curcumin loaded at different concentration in lipid bilayers of pure DMPC and mixtures of DPMC/TMCL. For spectrophotometry and fluorescence, we considered membrane model systems in the form of multilamellar lipid dispersions, known as liposomes, and hereafter referred to as lipid bilayers. They were prepared by using the thin film hydration method [31]. Proper amounts of the synthetic lipid powders were dissolved in chloroform/methanol (2:1 v/v). The organic solvent was evaporated first under a nitrogen gas stream and then under vacuum overnight. The dried films were fully hydrated at the concentration of 1.45 mM in DPBS by heating at $T = 35$ °C, and periodically vortexing. Titration experiments were performed by adding aliquots of curcumin, from 1 to 145 μM, from a stock solution (5×10^{-2} M) in ethanol to preformed bilayers. The samples were loaded in a quartz cell of 1 cm path length and left to equilibrate for 5 min at 25 °C before measuring. For any absorption spectrum, curcumin-free sample solution was loaded in the reference cell. In the case of lipid bilayers, the differential recording allows to eliminate the contribution due to the lipid scattering. UV–Vis absorption spectra were acquired over the range 250–450 nm by using a Cary 100 BioMelt spectrophotometer (Agilent Tech, USA) equipped with a 6 × 6 Peltier thermostated cell holder (accuracy ±0.3 °C).

2.3. Fluorescence

As for spectrophotometry, steady-state fluorescence measurements were executed on curcumin dissolved in various solvents at 15 μM or complexed with lipid bilayers, which were prepared as described above in paragraph 2.2. Fluorescence experiments with lipid bilayers were performed by varying the curcumin concentration (in the range 1–46 μM) at fixed bilayers concentration (1.45 mM), to determine the

association binding constant of the polyphenol to the lipid bilayers. After each curcumin addition, the sample was left to equilibrate for 5 min and finally the spectrum was recorded at 25 °C. All fluorescence data were collected on a LS 50B spectrofluorimeter (Perkin-Elmer, Beaconsfield, UK). For the curcumin intrinsic fluorescence, the excitation wavelength was fixed to 420 nm and the emission spectra recorded over the range 400–700 nm scanned at 200 nm/min. The width of excitation and emission slits was set at 6 and 4 nm, respectively. Each spectrum is the average of three successive scans.

2.4. Pressure-area isotherms and compressibility on Langmuir films

Langmuir films were produced in a clean room at room temperature by using a NIMA UK Pockels-Langmuir Trough (622 model) located under a laminar flow hood in order to reduce surface contamination. Surface tension measurements were carried out by means of the Wilhelmy plate technique. The subphase used for each experiment was Milli-Q grade deionized water.

All the compounds (lipids and curcumin) were dissolved at appropriate concentration in chloroform. DMPC and mixed DMPC/TMCL monolayers without and with different molar fractions of curcumin (2 or 10 mol%) were prepared at the air-water interface according to the Langmuir technique [32]. The appropriate amount of the compound solutions was spread by using a microsyringe onto the aqueous subphase; after the deposition, the solvent was allowed to evaporate before beginning the compression. Symmetric compression was achieved with two moving barriers at a constant rate of tens $Å^2$ min^{-1}. The surface pressure-area (π-A) isotherms were collected as a function of area/molecule. Compression and decompression isotherms were also acquired in order to check the monolayer stability and hysteresis. Information about the rheological properties of the monolayers, as well as information about thermodynamics and structural characteristics, has been obtained on the basis of a two-dimensional compressibility or compression modulus, $C_S^{-1} = -A(\partial\pi/\partial A)_{T,p,n}$, where the indices T, p and n indicate the constant temperature, pressure and composition of the monolayer, respectively [33].

2.5. Atomic force microscopy

The pure and mixed phospholipid monolayers in the absence and in the presence of curcumin studied by AFM were prepared as described above, in the paragraph 2.4. They were deposited at onto freshly cleaved mica substrate, at two different surface pressures of 20 mN/m and 25 mN/m. Topographic images of Langmuir thin films were acquired by using a Bruker Multimode 8 AFM equipped with a Nanoscope V controller. Measurements were carried out in Peak Force mode at room temperature, at least one day after the monolayer deposition, to allow complete water evaporation. Silicon cantilevers (model RTESPA-300, Burker) with 10 nm tip radius and 42 N/m elastic constant were used to acquire the AFM images, with a scan rate of 0.7 Hz. To analyze the images and evaluate the topographic features, both the freely distributed analysis software Gwyddion (GNU General Public License) [34] and the Nanoscope Analysis software (Bruker) have been used.

In any given experiment, two independent measurements were executed to test their reproducibility.

3. Results and discussion

3.1. Spectrophotometric and fluorescence measurements

3.1.1. Solvatochromic properties of curcumin in solvents and lipid bilayers

In order to investigate the association of curcumin with lipid membranes and to assess its preferred anchoring region within the bilayers, UV–vis and fluorescence spectra of curcumin when it is dissolved in solvents with different dielectric constant (i.e., polarity) or bound to lipid bilayers of DMPC or DMPC +4 mol% TMCL were recorded at 25 °C. According to previous studies, the incorporation of low TMCL content had no major effect on the DMPC main phase transition temperature, that is reported to occur at ca. 24 °C [29,30]. This ensures that the lipid bilayers are in the fluid state and the presented results are not affected by the lipid sample composition. In agreement with literature data [13,35,36], the absorption spectrum of curcumin in DPBS (see Fig. 2 and inset) consists of a broad band with a maximum at $\lambda_{max} = 427$ nm and a shoulder at ca. 350 nm.

A progressive reduction of the bandwidth and a blue shift of λ_{max} are observed upon decreasing the solvent polarity. Indeed, λ_{max} decreases to 422 nm in ethanol, it is 419 nm in methanol and 417 nm in acetonitrile, and the spectrum is downshifted at ca. 408 nm when the ligand is dissolved in the apolar solvent n-hexane. The absorption spectra of curcumin show shoulders for $\lambda > \lambda_{max}$ in methanol and to a lesser extent in acetonitrile and at lower and higher wavelength in the case of n-hexane. Solvent dependent absorption maxima of curcumin characterized by blue shift in less polar solvents are reported in literature [37]. The absorption spectra of curcumin in DMPC and DMPC/TMCL bilayers display a shape rather similar to that in ethanol or methanol with shoulders at $\lambda > \lambda_{max}$ (see Fig. 2 and inset).

The fluorescence spectrum of curcumin in DPBS is a structureless low intensity peak at $\lambda_{em} \approx 528.5$ nm; it intensifies and, in line with the

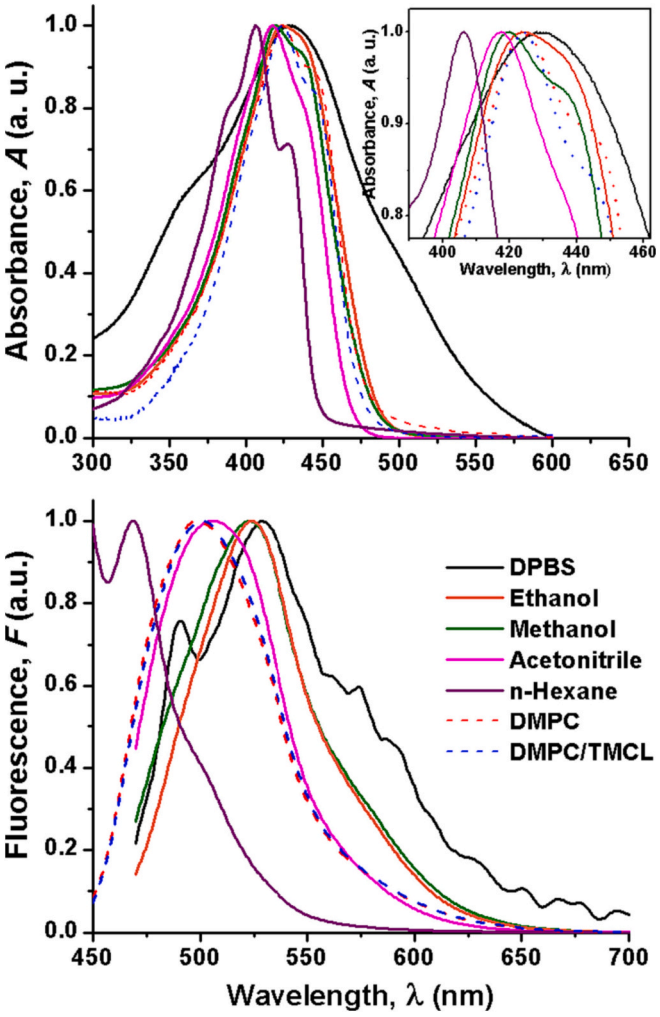

Fig. 2. Absorption and fluorescence spectra at 25 °C of 15 μM curcumin in (solid lines) various solvents and in (dashed lines) 1.45 mM aqueous dispersions of lipid bilayers. Spectra are normalized at the same height. The inset shows a zoom of the spectra in the region of maximum absorption to improve visualization.

UV–Vis spectra, undergoes a blue shift from ca. 525 nm in ethanol and methanol, to ca. 506 nm in acetonitrile, and to 500 nm in acetone (see Fig. 2). These solvatochromic shifts are in close agreement with previous determinations [36]. It is interesting to observe from Fig. 2 that somewhat similar spectra with $\lambda_{em} \approx 500$ nm are obtained for curcumin in DMPC and DMPC/TMCL bilayers.

The UV–Vis and fluorescence results clearly indicate that the ligand interacts with the bilayers, anchors at the polar/apolar interfaces and locates in the hydrophobic region of the first $-CH_2$ acyl chain segments in both DMPC and DMPC/TMCL matrices. The presence of TMCL favors the association of curcumin to the lipid bilayers. Curcumin partitioning from the polar environment of the aqueous buffer to the non-polar region of phosphocholine vesicles has been reported [38]. By using semiempirical models of solvatochromic shifts to predict the location of fluorophore in lipid bilayer, it has been estimated that curcumin is at 1–1.2 nm from the phospholipid/water interface, in the acyl chain region of lipid bilayer [39]. In close agreement with our results, a joint spectrophotometric and fluorescence investigation reported that curcumin is associated in the hydrocarbon zone of DPPC bilayers [35]. Also, fluorescence quenching experiments showed that curcumin locates preferentially in the hydrophobic acyl chain region of egg yolk phosphatidylcholine (EYPC), close to the glycerol group of the lipid molecules [13]. Literature data report that the polar/apolar interface is the preferred anchoring region of Cur in lipid bilayers [16,17] and indicate that CL (from bovine heart) in biomimetic and biological mitochondrial membranes assists Cur insertion into the bilayer core and, particularly, in the headgroup region [16]. It is likely that, through nonspecific interactions and anchored by hydrogen bonding between its hydroxyl group and the phosphate group of DMPC, the amphipathic curcumin accommodates into the lipid bilayers in a transmembrane orientation in a manner analogous to cholesterol and amphipathic peptides, as previously suggested [11,12].

3.1.2. *Binding constant of curcumin to lipid bilayers*

To evaluate the binding constant of the polyphenol to the lipid bilayers, UV–vis absorption and fluorescence spectra of lipid bilayer/curcumin complexes have been recorded as a function of curcumin concentration at fixed liposome concentration (see Fig. 3).

From the UV–Vis spectra in Fig. 3 – upper panel, it can be seen that, for both DMPC and DMPC/TMCL bilayers, the absorbance increases on increasing curcumin concentration but to a slightly different extent. Similarly, the fluorescence intensity increases differently on titrating curcumin on DMPC and DMPC/TMCL bilayers (Fig. 3 – lower panel). The absorbance and fluorescence intensity increase as well as the blue shift of the spectra indicate the binding of Cur to the lipid bilayers.

From the above data the binding constant, K_a, of the drug to the lipid bilayers can be evaluated according to the Benesi–Hildebrand equation [13,35,40,41]:

$$\frac{1}{P} = \frac{1}{l\Delta\varepsilon[L]_0 K_a}\frac{1}{[Cur]} + \frac{1}{l\Delta\varepsilon[L]_0} \quad (1)$$

where P is the absorbance, A, or the fluorescence, F, at any point of the binding process, $\Delta\varepsilon$ is the differential extinction coefficient, l is the optical path length, $[L]_0$ is the constant lipid concentration and [Cur] is the curcumin concentration. The binding constants were determined from the linear fit of the reciprocal plots of the change in A or F of the lipid/curcumin solution as a function of curcumin concentration. The obtained K_a values are reported in Table 1 along with the free energy of binding $\Delta G = -RTlnK_a$.

On the whole, the K_a determinations show consistency each other in

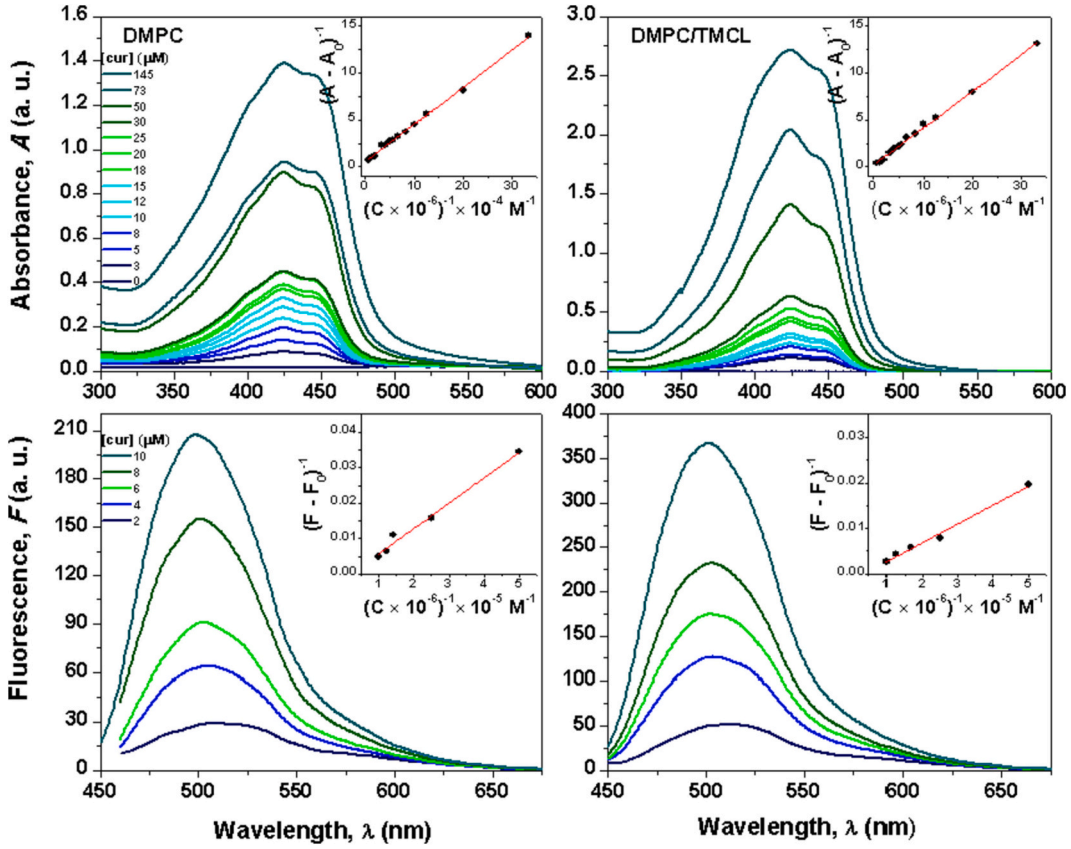

Fig. 3. UV–Vis (upper panel) and fluorescence (lower panel) spectra of curcumin at different concentration in DMPC and in DMPC/TMCL bilayers (1.45 mM). *Insets*. Double reciprocal plots of the absorbance, A, or fluorescence, F, versus curcumin concentration, and fitted lines according to eq. (1) for curcumin in DMPC and DMPC/TMCL bilayers.

Table 1
Binding constants, K_a, and free energy of binding, ΔG, for curcumin to DMPC and DMPC/TMCL bilayers derived from the linear fits according to Eq. (1) of the UV–vis and fluorescence data reported in the insets to Fig. 3.

Bilayers	UV–Vis		Fluorescence	
	$K_a \cdot 10^4$ (M^{-1})	ΔG (kcal M^{-1})	$K_a \cdot 10^4$ (M^{-1})	ΔG (kcal M^{-1})
DMPC	0.56 ± 0.22	−5.12 ± 0.23	1.47 ± 0.48	−5.69 ± 0.19
DMPC/TMCL	1.45 ± 0.24	−5.68 ± 0.10	3.30 ± 1.62	−6.17 ± 0.29

that they are always higher in the presence of cardiolipin and indicate that curcumin has a slightly higher affinity for DMPC/TMCL than for pure DMPC bilayers. Moreover, the K_a values are comparable to those reported for the association of small ligands and drugs to lipid assemblies of various compositions, including curcumin to EYPC bilayers [13] and warfarin to neutral, anionic and cationic lipid bilayers [42]. For comparison, it is interesting to note that the determined association constants for curcumin-membranes are slightly lower than that found for the binding of this ligand to carrier proteins such as albumin [35].

3.2. Surface tension and compressibility measurements on Langmuir monolayers

Over decades, surface-tension measurements have been the main source of information about insoluble monolayers since the study of the (π–A) isotherms under equilibrium conditions allows not only to determine monolayer elasticity but also the equations of state. The compressibility properties of Langmuir monolayers deduced from (π–A) isotherms can provide information about thermodynamics and structural characteristics, such as the presence of several phase transitions, (G – gaseous, LE – liquid expanded, LC – liquid condensed, S – solid) whose compressibility follow the sequence G > LE > LC > S [43]. The collapse pressure, instead, is a key parameter to test the miscibility of two or more compounds.

(π–A) isotherms have been acquired on either DMPC or DMPC/TMCL films in the absence and in the presence of 2 or 10 mol% of Cur. Pure curcumin does not form stable monolayers at the air-water interface [44]. In Figs. 4 A and B are reported the compressibility data, i.e., C_S^{-1} vs π, of the monolayers at the working temperature.

Pure DMPC displays a LE phase, as reported in literature [45]. TMCL is miscible with DMPC; in fact, the DMPC/TMCL monolayer collapse pressure increases (~ 45 mN/m) and a region of LC phase is observed (see Fig. 4). The increase of the collapse pressure has been used to indicate complete miscibility for DPPC/cardiolipin [46] and EYPC/cardiolipin [47] monolayers at all the molar ratios investigated. The collapse pressure increases as well when low molar concentration of curcumin (2% mol) is added in DMPC (~47 mN/m) and even more in DMPC/TMCL monolayers (~50 mN/m) (Fig. 4A). A quite distinct behavior is observed in the monolayers doped with curcumin at 10 mol %. Indeed, curcumin at this content downshifts the collapse pressure at 40 mN/m in DPMC and at 45 mN/m in DMPC/TMCL. Nevertheless, a LE/LC transition is observed in both samples (Fig. 4B). The findings on compressibility in Fig. 4 indicate that the addition of TMCL in DMPC induces the formation of a more compact monolayer, in contrast with the reported increase of the liquid expanded region and elasticity upon adding a higher content of cardiolipin to DPPC [48]. The three component systems show a condensing effect at low Cur molar percentage, i.e. Cur favors the molecular packing, whereas a reduced overall monolayer stability is seen at high Cur molar percentage. A condensing and stiffening effect of curcumin was previously reported on EYPC monolayers [13] and on DPPC films [49]. This finding is in agreement with nuclear magnetic resonance and differential scanning calorimetry results obtained by Ramamoorthy and coworkers showing that curcumin at low concentrations has an ordering effect on the DMPC or DPPC membrane structure [12].

More insights on the molecular packing at the interface can be gained by considering the fractional area/molecule variation, $\Delta A/A$, that can occur when an "addendum" X is added to a matrix film M, defined by:

$$(\Delta A/A)_{M+X} = (A_{M+X} - A_M)/A_M$$

According to this definition, a negative $\Delta A/A$ value is obtained when the area per molecule of the matrix + the addendum X, A_{M+X}, is lower than the area per molecule of the pure matrix, A_M. Therefore, a negative $\Delta A/A$ value indicates that the addendum X is completely incorporated or intercalated in the monolayer, while a low $\Delta A/A$ value indicates a pretty well incorporation or intercalation of the addendum in the monolayer.

Considering the pure matrices, the area per molecules of DMPC/TMCL isotherm increases noticeably with respect to pure DMPC $\left((\Delta A/A)_{DMPC+TMCL} \approx 40 - 45\%\right)$ (data not shown), indicating that the lipids are arranged in monolayers at the interfaces, as occurred for DPPC and TMCL in Langmuir monolayers [48].

In Fig. 5 we report $\Delta A/A$ for DMPC and DMPC/TMCL monolayers with 2 or 10 mol% curcumin.

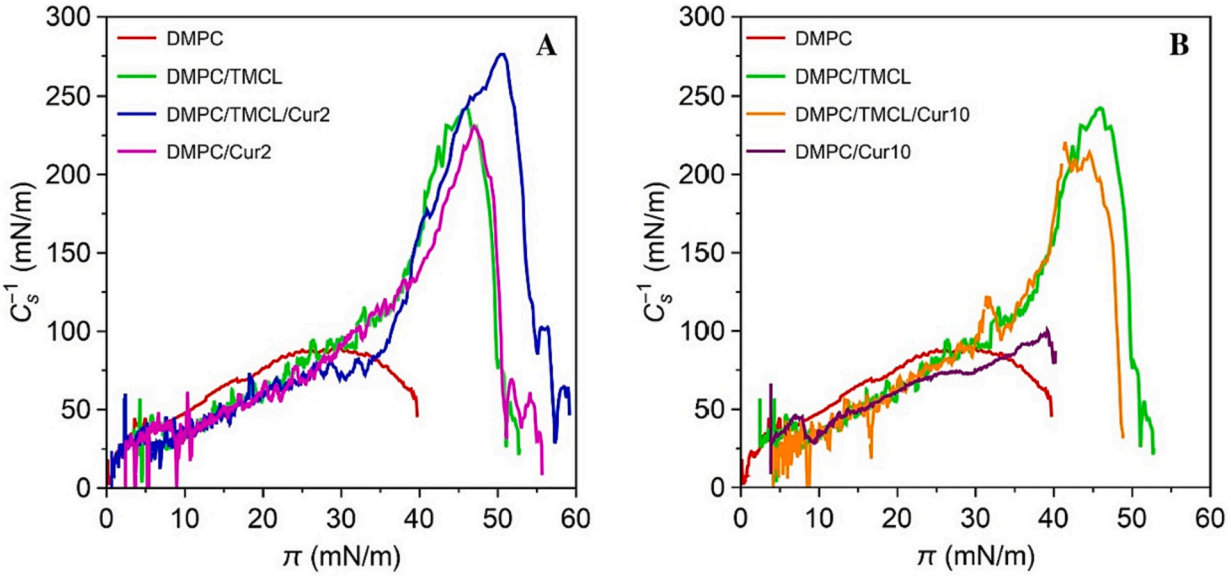

Fig. 4. Compression modulus versus pressure of Langmuir films of DMPC and DMPC/TMCL with curcumin at (A) 2 mol% and (B) 10 mol%.

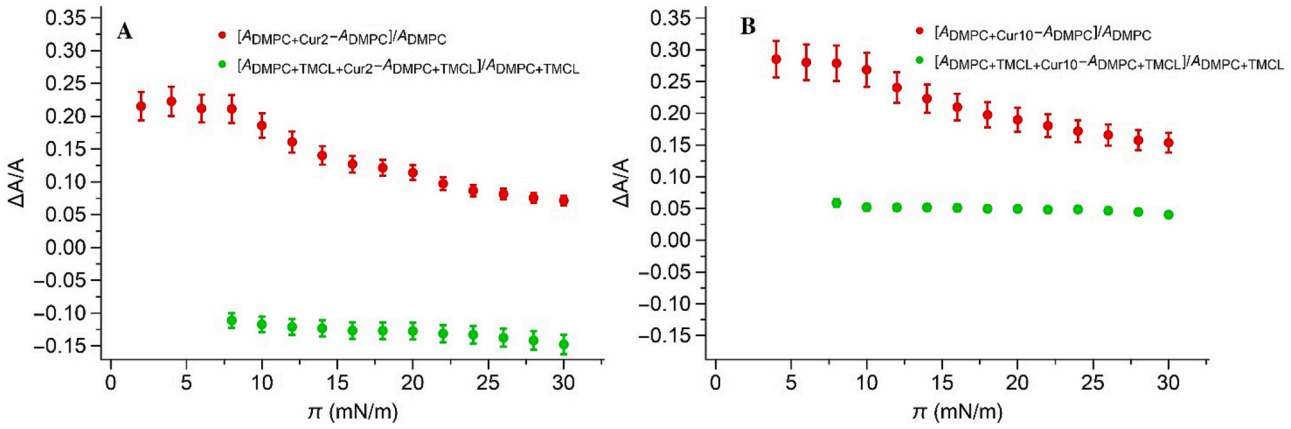

Fig. 5. Fraction of area variation as a function of pressure of Langmuir films of DMPC and DMPC/TMCL with curcumin at (A) 2 mol% and (B)10 mol%.

At low pressure, the area variations $(\Delta A/A)_{DMPC+Cur2}$ and $(\Delta A/A)_{DMPC+Cur10}$ are ≈ 20% and ≈ 30%, respectively. The addition of curcumin at 10 mol% probably induces a higher packing density of molecules at air/water interface or the formation of Cur aggregates in the monolayers, as the lowering of the collapse pressure suggests (see Fig. 4B).

Considering the ternary systems, the $(\Delta A/A)_{DMPC/TMCL+Cur2}$ and $(\Delta A/A)_{DMPC/TMCL+Cur10}$ data in Fig. 5 suggest a strong interaction among the components. It is likely that 2 mol% of Cur are better incorporated in the monolayer $((\Delta A/A)_{DMPC/TMCL+Cur2} < 0)$ than 10 mol% of Cur $((\Delta A/A)_{DMPC/TMCL+Cur10}) > (\Delta A/A)_{DMPC/TMCL+Cur2})$; moreover, by comparing the data reported in Fig. 5, Cur at 10 mol% is better incorporated in cardiolipin-containing monolayers with respect to pure DMPC. These results clearly indicate that TMCL promotes the incorporation of higher concentration of Cur in the phospholipid matrix.

3.3. Atomic force microscopy measurements

A more in-depth characterization of the interactions among lipids and curcumin can be made by analyzing the morphology of DMPC and DMPC/TMCL monolayers when doped with Cur. This has been done by collecting AFM topographic images of the Langmuir films deposited on mica at two pressures, namely 20 mN/m and 25 mN/m, quite below the critical collapse ones. In Fig. 6 we report the topographies of pure and doped monolayers at a pressure of 25mN/m. We observed no changes in the topographic features for the same samples deposited at 20mN/m (data not reported).

From the AFM images it can be observed that the addition of 2 mol% of Cur to pure DMPC (Fig. 6 b) slightly alters the morphology of the pure DMPC monolayer (Fig. 6a) in terms of "higher coverage" of the substrate. However, Cur does not affect neither the height, h, nor the roughness, R_q, of the monolayers that are almost comparable in the two samples (see Table 2). A drastic change in the morphology is observed

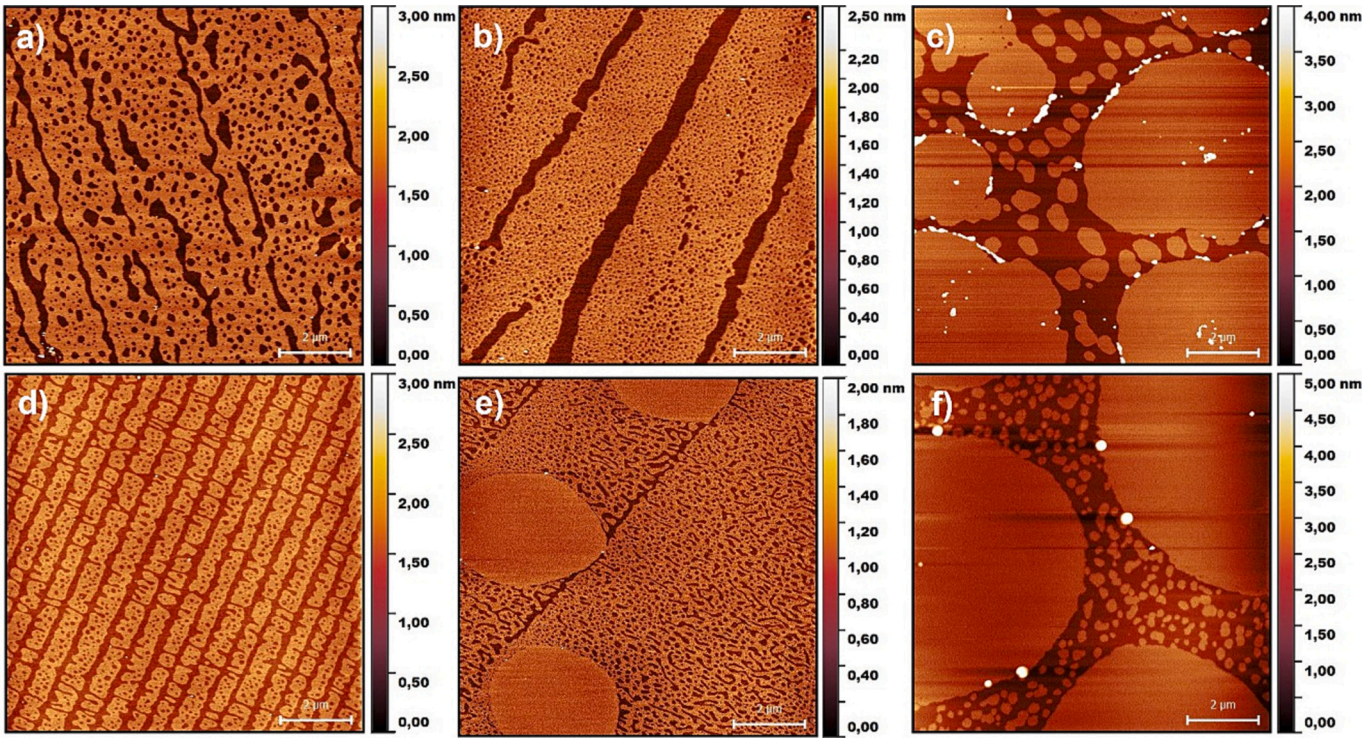

Fig. 6. AFM topography of Langmuir films deposited onto freshly cleaved mica at a pressure of 25 mN/m of a) DMPC; b) DMPC+ 2 mol% Curcumin; c) DMPC+ 10 mol% Curcumin; d) DMPC/TMCL; e) DMPC/TMCL+2 mol% Curcumin; f) DMPC/TMCL+10 mol% Curcumin. The scale bar is 2 μm.

Table 2
Height, h, and surface roughness, R_q, for Langmuir films deposited on mica at a pressure of 25mN/m of DMPC and DMPC/TMCL with curcumin at 2 mol% and 10 mol%.

Sample	h(nm)	R_q(nm)
DMPC	0.91 ± 0.20	0.43 ± 0.10
+ 2 mol% Cur	0.84 ± 0.13	0.37 ± 0.20
+ 10 mol% Cur	1.03 ± 0.23	0.66 ± 0.30
DMPC/TMCL	0.77 ± 0.13	0.30 ± 0.20
+ 2 mol% Cur	0.98 ± 0.12	0.25 ± 0.20
+ 10 mol% Cur	1.30 ± 0.80	0.45 ± 0.20

when 10 mol% of curcumin is added to the pure DMPC matrix (Fig. 6c). Indeed, from Fig. 6c it can be seen that the curcumin addition gives rise to both large and small terraces sometimes surrounded by bright spots. These latter can be ascribed to an excess of curcumin that is not incorporated in the lipid matrix, as also noted from area/molecule variation presented above. Moreover, for Fig. 6c the height (h = 1.03 ± 0.23 nm) and the roughness (R_q 0.66 ± 0.30 nm) of the monolayers increase if compared with the previous ones. Similar changes in morphology due to the presence of Cur were reported for DPPC monolayers [19]. Moreover, curcumin concentration-dependent topography variations were also observed for DOPC membranes: whereas low curcumin content does not alter the global organization of the membrane, higher amount induces structure reorganization [50].

Fig. 6d shows the topography of DMPC doped with 4 mol% of TMCL. Looking at the morphological features, it seems that the presence of cardiolipin stabilizes in some way the coverage of the substrate, slightly decreasing the height and the roughness of the monolayer compared to the pure DMPC (compare Fig. 6a and d and see Table 2). This is a confirmation of our compressibility data that DMPC and low amount of TMCL are well miscible in the monolayers. In agreement with our results, a reduction of terrace heights and roughness has also been shown by AFM in various lipid monolayers upon cardiolipin inclusion [46,51]. Results obtained by Tristram-Nagle and coworkers indicated that TMCL thickens and stiffens DMPC membranes, orders chains, and is positioned under the umbrella of the PC headgroup [29]. Higher content of TMCL (> 5 mol%) was found to promote the formation of areas with apposed double bilayers or nonlamellar structures within EYPC membrane [14].

Remarkable curcumin concentration-dependent morphological features are observed in DMPC/TMCL films. For Cur at 2 mol%, small islands start to appear, almost not affecting neither the height or the roughness of the monolayer (compare Fig. 6d and e and the corresponding data in Table 2). For Cur at 10 mol% (Fig. 6f) large terraces surrounded by very small ones and only few aggregates are evident as well as a further slight increase of both the height and the roughness of the films (compare Fig. 6e and f and the corresponding data in Table 2). The most likely explanation of the lack of the aggregates surrounding the terraces in DMPC/TMCL films relative to those of DMPC is that TMCL helps the incorporation of curcumin inside the phospholipid assemblies, resulting in an increase of the terrace area and height and in a decrease of the roughness. The overall AFM topographic images and the h and R_q determinations clearly indicate that Cur preferentially associates with cardiolipin-containing monolayers; this holds especially at low content, and it is likely that curcumin is positioned at the lipid polar-heads, as the reduction of the roughness relative to the Cur addition to DMPC suggests. Similarly, it has been found that CL (from bovine heart) promoted the adsorption and internalization of curcumin into model and mitochondrial membranes, with pronounced uptake into the headgroup area of DMPC vesicles [16].

4. Conclusions

By combining several experimental techniques, the interaction of curcumin with model systems of mitochondrial membranes have been investigated. Fully hydrated bilayers and monolayers at the air/water interface as well as supported on mica surface composed of pure DMPC or mixtures of DMPC and 4 mol% of TMCL with identical chain length have been considered. The most relevant results can be summarized as follows. Curcumin associates at the first acyl chain segments of both pure DMPC and mixed DMPC/TMCL bilayers and the free energy of binding is more favorable in the presence of cardiolipin. Our compressibility and AFM data provide original insight on the interaction of curcumin with DMPC and DMPC/TMCL monolayers. DMPC lipids mix well with TMCL. Pure and mixed monolayers are miscible with low content (2 mol%) of curcumin which is better incorporated in the presence of cardiolipin. Interestingly, at variance with what seen in DMPC, the presence of cardiolipin also favors the intercalation of high content (10 mol%) of curcumin, reducing the aggregates and inducing the formation of compact terraces. Such an effect of cardiolipin could be ascribed to its ability to induce membrane alterations that support the role of CL in facilitating bilayer structure remodeling, deformation, and permeabilization, as reported by a study on the effects of CL on various types of lipid membranes [14]. Our findings on the interplay cardiolipin-curcumin in affecting membrane properties have a twofold relevance. They indicate that cardiolipin-based model membranes represent a biocompatible platform to inglobate the water-insoluble curcumin and contribute to the optimization of the design of efficient drug-delivery systems to be used “in-vivo”. The results also highlight the preferential effect of curcumin on the mitochondrial membranes, that is important for the therapeutic role of the molecule in mitochondrial membranes related physiopathologies.

Credit author statement

All the authors designed research; R.B. supervised the research; E.A. performed Uv-vis and fluorescence experiments; F.C. performed Langmuir experiments; C.M.T. performed AFM measurements; E.A., C.M.T., F.C., R.B. analyzed data; C.M.T., F.C., R.B. wrote the first draft; R.B. and C.M.T. wrote the manuscript (review & editing); R.C.B. financially supported the research; all the authors read and approved the manuscript.

Declaration of Competing Interest

The authors declare that they have no known competing financial interests or personal relationships that could have appeared to influence the work reported in this paper.

Acknowledgments

C.M.T. acknowledges PON “Attraction and International Mobility” R&I 2014 – 2020, AIM 1875705-2, CUP H24119000450005 and PON “Ricerca e Innovazione” 2014-2020, CUP H25F21001220006. The authors thank Maria Luisa Amoroso for help at the early stage of the experimental work.

References

[1] K.I. Priyadarsini, The chemistry of curcumin: from extraction to therapeutic agent, Molecules 19 (2014) 20091–20112.
[2] H. Hatcher, R. Planalp, J. Cho, F.M. Torti, S.V. Torti, Curcumin: from ancient medicine to current clinical trials, Cell. Mol. Life Sci. 65 (2008) 1631–1652.
[3] J. Sharifi-Rad, Y. El Rayess, et al., Turmeric and its major compound curcumin on health: bioactive effects and safety profiles for food, pharmaceutical, biotechnological and medicinal applications, Front. Pharmacol. 11 (2020) 01021.
[4] S. Bose, A.K. Panda, S. Mukherjee, G. Sa, Curcumin and tumor immune-editing: resurrecting the immune system, Cell Div 106 (2015).
[5] K.H. Jung, J.H. Lee, J.W. Park, S.H. Moon, Y.S. Cho, Y.S. Choe, K.H. Lee, Effects of curcumin on cancer cell mitochondrial function and potential monitoring with ^{18}F-FDG uptake, Oncol. Rep. 35 (2016) 861–868.
[6] S. Abrahams, W.L. Haylett, G. Johnson, J.A. Carr, S. Bardien, Antioxidant effects of curcumin in models of neurodegeneration, aging, oxidative and nitrosative stress: a review, Neuroscience 406 (2019) 1–21.

[7] A. Hesari, M. Azizian, et al., Chemopreventive and therapeutic potential of curcumin in esophageal cancer: current and future status, Int J Cancer 144 (2019) 1215–1226.
[8] A. Mohammadi, A.H. Colagar, A. Khorshidian, S.M. Amini, The functional roles of curcumin on astrocytes in neurodegenerative diseases, Neuroimmunomodulation 29 (2022) 4–14.
[9] B. Zheng, D.J. McClement, Formulation of more efficacious curcumin delivery systems using colloid science: enhanced solubility, stability, and bioavailability, Molecules 25 (2020) 2791.
[10] K. Gardikis, S. Hatziantoniou, K. Viras, C. Demetzos, Effect of a bioactive curcumin derivative on DPPC membrane: a DSC and Raman spectroscopy study, Thermochim. Acta 447 (2006) 1–4.
[11] Y. Sun, C.-C. Lee, W.-C. Hung, F.-Y. Chen, M.-T. Lee, H.W. Huang, The bound states of amphipathic drugs in lipid bilayers: study of curcumin, Biophys. J. 95 (2008) 2318–2324.
[12] J. Barry, M. Fritz, J.R. Brender, P.E.S. Smith, D.K. Lee, A. Ramamoorthy, Determining the effects of lipophilic drugs on membrane structure by solid-state NMR spectroscopy: the case of the antioxidant curcumin, J. Am. Chem. Soc. 131 (2009) 4490–4498.
[13] A. Karewicz, D. Bielska, B. Gzyl-Malcher, M. Kepczynski, R. Lachc, M. Nowakowska, Interaction of curcumin with lipid monolayers and liposomal bilayers, Coll Surf B 88 (2011) 231–239.
[14] J.D. Unsay, K. Cosentino, Y. Subburaj, A.J. García-Sáez, Cardiolipin effects on membrane structure and dynamics, Langmuir 29 (2013) 15878–15887.
[15] M. Tsukamoto, et al., Modulation of raft domains in a lipid bilayer by boundary-active curcumin, Chem. Commun. 50 (2014) 3427–3430.
[16] S. Ben-Zichri, S. Kolusheva, M. Danilenko, S. Ossikbayeva, W.J. Stabbert, J. L. Poggio, D.E. Stein, Z. Orynbayev, R. Jelinek, Cardiolipin mediates curcumin interactions with mitochondrial membranes, Biochim. Biophys. Acta Biomembr. 2019 (1861) 75–82.
[17] M. Duda, K. Cygan, A. Wisniewska-Becker, Effects of curcumin on lipid membranes: an EPR spin-label study, Cell Biochem. Biophys. (2020).
[18] N. Civelek, D. Bilge, Investigating the molecular effects of curcumin by using model membranes, Food Biophys 17 (2022) 232–247.
[19] M. Pedrosa, J. Maldonado-Valderrama, M.J. Galvez-Ruiz, Interactions between curcumin and cell membrane models by Langmuir monolayers, Colloids Surf. B: Biointerfaces 217 (2022), 112636.
[20] G. Van Meer, D.R. Voelker, G.W. Feigenson, Membrane lipids: where they are and how they behave, Nat. Rev. Mol. Cell Biol. 9 (2008) 112–124.
[21] Z. Yang, L. Wang, C. Yang, S. Pu, Z. Guo, Q. Wu, Z. Zhou, H., Zhao mitochondrial membrane remodeling. Front Bioeng, Biotechnol 9 (2022), 786806.
[22] H. Bagheri, Effects of curcumin on mitochondria in neurodegenerative diseases, Biofactors 46 (2020) 5–20.
[23] H. Tabassum, S. Parvez, Curcumin and mitochondria, in mitochondrial physiology and vegetal molecules, in: Therapeutic Potential of Natural Compounds on Mitochondrial Health, 2021, pp. 439–454. Chapter 20.
[24] X. Li, J. Zhu, Q. Lin, M. Yu, J. Lu, J. Feng, C. Hu, Effects of curcumin on mitochondrial function, endoplasmic reticulum stress, and mitochondria-associated endoplasmic reticulum membranes in the jejunum of oxidative stress piglets, J. Agric. Food Chem. 70 (2022) 8974–8985.
[25] F.J. Sala de Oyanguren, N.E. Rainey, A. Moustapha, A. Saric, F. Sureau, J.-E. O'Connor, P.-X. Petit, Highlighting curcumin-induced crosstalk between autophagy and apoptosis as supported by its specific subcellular localization, Cells 9 (2020) 361.
[26] M. Zheng, Q. Zhang, Y. Joe, B.H. Lee, D.G. Ryu, K.B. Kwon, S.W. Ryter, H.T. Chung, Curcumin induces apoptotic cell death of activated human CD4+ T cells via increasing endoplasmic reticulum stress and mitochondrial dysfunction, Int. Immunopharmacol. 15 (2013) 517–523.
[27] A. Shakeri, M.R. Zirak, A.W. Hayes, R. Reiter, G. Karimib, Curcumin and its analogues protect from endoplasmic reticulum stress: mechanisms and pathways, Pharm. Res. 146 (2019), 104335.
[28] R.N.A.H. Lewis, R.N. McElhaney, The physicochemical properties of cardiolipin bilayers and cardiolipin-containing lipid membranes, Biochim. Biophys. Acta 1788 (2009) 2069–2079.
[29] A.L. Boscia, B.W. Treece, D. Mohammadyani, J. Klein-Seetharaman, A.R. Braun, T. A. Wassenaar, B. Klösgen, S. Tristram-Nagle, X-ray structure, thermodynamics, elastic properties and MD simulations of cardiolipin/dimyristoylphosphatidylcholine mixed membranes, Chem. Phys. Lipids 178 (2014) 1–10.
[30] E.R. Pennington, A. Fix, E.M. Sullivanan, D.A. Brown, A. Kennedy, S.R. Shaikh, Distinct membrane properties are differentially influenced by cardiolipin content and acyl chain composition in biomimetic membranes, Biochim Biophys Acta 1859 (2017) 257–267.
[31] D.D. Lasic, Liposomes: From Physics to Applications, Elsevier Science Limited, Amsterdam, 1993.
[32] G. Roberts, Langmuir-Blodgett Films, Plenum Press, New York, 1990.
[33] T. Davies, E.K. Rideal, Interfacial Phenomena, Academic Press, New York, 1963.
[34] D. Nečas, P. Klapetek, Gwyddion: an open-source software for SPM data analysis, cent, Eur. J. Phys. 10 (2012) 181–188.
[35] A. Kunwar, A.B. Pandey, K.I. Priyadarsini, Transport of liposomal and albumin loaded curcumin to living cells: an absorption and fluorescence spectroscopic study, Biochim. Biophys. Acta 1760 (2006) 1513–1520.
[36] S. Mondal, G. Soumen, S.P. Moulik, Stability of curcumin in different solvent and solution media: UV–visible and steady-state fluorescence spectral study, J. Photochem. Photobiol. B Biol. 158 (2016) 212–218.
[37] A. Majhi, G.M. Rahman, S. Panchal, J. Das, Binding of curcumin and its long chain derivatives to the activator binding domain of novel protein kinase C, Bioorg. Med. Chem. 18 (2010) 1591–1598.
[38] N.B. Leite, D.B. Martins, V.E. Fazani, M.R. Vieira, M.P. dos Santos Cabrera, Cholesterol modulates curcumin partitioning and membrane effects, Biochim. Biophys. Acta Biomembr. 1860 (2018) 2320–2328.
[39] E.G. Randles, P.R. Bergethon, Reaction field analysis and lipid bilayer location for lipophilic fluorophores, J. Phys. Chem. B 117 (35) (2013) 10193–10202.
[40] I.D. Kuntz, F.P. Gasparro, M.D. Johnston, R.P. Taylor, Molecular interactions and the Benesi-Hildebrand equation, J. Am. Chem. Soc. 90 (1968) 4778–4781.
[41] O. Exner, Calculating equilibrium constant from spectral data: reliability of the Benesi–Hildebrand method and its modifications, Chemom. Intell. Lab. Syst. 39 (1997) 85.
[42] E. Aloi, B. Rizzuti, R. Guzzi, R. Bartucci, Binding of warfarin differently affects the thermal behavior and chain packing of anionic, zwitterionic and cationic lipid membranes, Arch. Biochem. Biophys. 694 (2020), 108599.
[43] D. Vollhardt, V.B. Fainerman, Progress in characterization of Langmuir monolayers by consideration of compressibility, Adv. Colloid Interf. Sci. 127 (2006) 83–97.
[44] M. Girardon, B. Korchowiec, J. Korchowiec, E. Rogalskaa, N. Canilho, A. Pasc, A way to introducing a hydrophilic bioactive agent into model lipid membranes. The role of cetyl palmitate in the interaction of curcumin with 1,2-dioleoyl-sn-glycero-3-phosphatidylcholine monolayers, J. Mol. Liq. 308 (2020), 113040.
[45] J. Mascetti, S. Castano, D. Cavagnat, B. Desbat, Organization of β-Cyclodextrin under pure cholesterol, DMPC, or DMPG and mixed cholesterol/phospholipid monolayers, Langmuir 24 (2008) 9616–9622.
[46] S. Sennato, F. Bordi, C. Cametti, C. Coluzza, A. Desideri, S. Rufini, Evidence of domain formation in cardiolipin−glycerophospholipid mixed monolayers. A thermodynamic and AFM study, J. Phys. Chem. B 109 (2005) 15950–15957.
[47] S. Nichols-Smith, S.Y. Teh, T.L. Kuhl, Thermodynamic and mechanical properties of model mitochondrial membranes, Biochim. Biophys. Acta 1663 (2004) 82–88.
[48] M.D. Phan, K. Shin, Effects of cardiolipin on membrane morphology: a Langmuir monolayer study, Biophys. J. 108 (2015) 1977–1986.
[49] G. Xu, C. Hao, L. Zhang, R. Sun, Investigation of surface behavior of DPPC and curcumin in Langmuir monolayers at the air-water interface, Scanning (2017) (Article ID 6582019).
[50] E. Arab-Tehrany, K. Elkhoury, G. Francius, L. Jierry, J.F. Mano, C. Kahn, M. Linder, Curcumin loaded Nanoliposomes localization by nanoscale characterization, Int. J. Mol. Sci. 21 (2020) 7276.
[51] S. Lopes, C.S. Neves, P. Eaton, P. Gameiro, Cardiolipin, a key component to mimic the E. coli bacterial membrane in model systems revealed by dynamic light scattering and steady-state fluorescence anisotropy, Anal. Bioanal. Chem. 398 (2010) 1357–1366.